Momentum transfer dependence behaviors of ionization and dissociation of oxygen*

Lin Mei(林 梅)[a], Liu Ya-Wei(刘亚伟)[a], Zhong Zhi-Ping(钟志萍)[b], and Zhu Lin-Fan(朱林繁)[a]†

[a] Hefei National Laboratory for Physical Sciences at Microscale, Department of Modern Physics, University of Science and Technology of China, Hefei 230026, China

[b] School of Physical Sciences, University of the Chinese Academy of Sciences, P. O. Box 4588, Beijing 100049, China

(Received 10 June 2012; revised manuscript received 23 July 2012)

The decay pathways of the structured ionization region of oxygen at different momentum transfers, i.e., 0, 0.23 a.u. (atomic unit), and 0.91 a.u., are studied by measuring the ion and the scattered electron coincidently. It is found that the dipole-forbidden superexcited states of $(2\sigma_u)^{-1}(c^4\Sigma_u^-)np\sigma_u\ ^3\Sigma_g^- \leftarrow X^3\Sigma_g^-$ decay into different channels according to the principal quantum number n. The broad ridge above 35 eV, which may be due to inner-valence excited states of $(2\sigma_g)^{-1}n\lambda$ or multiply excited states, is observed both at small and large momentum transfers, and its decay channel of $O^+ + O$ is dominant.

Keywords: oxygen, superexcited states, ionization continuum, decay channel

PACS: 34.80.Gs, 33.80.Eh, 32.70.Cs, 33.20.Ni **DOI:** 10.1088/1674-1056/22/2/023404

1. Introduction

Oxygen is one of the major components of the Earth's atmosphere, and it plays an important role in a variety of combustion and energy conversion processes as well as in the atmospheric chemistry of the Earth. Besides, oxygen is the key element in respiration. Therefore, the cross sections of the ionization and dissociation of the "structured" ionization region, which extends from the first ionization threshold to about 20 eV, of O_2 are of great significance in many fields such as atmospheric chemistry, plasma physics, astrophysics, etc. On the other hand, as an open-shell diatomic molecule, oxygen has attracted the attentions of both theorists and experimentalists from the viewpoints of pure physics and chemistry.

In the collision processes of an electron with a molecule, direct ionization (formula (1)) and super-excitation (formula (2)) will occur if the energy transfer of the incident electron to the molecule exceeds the ionization threshold:

$$e_i + AB \rightarrow e_s(\theta) + [AB^{n+}]^j + ne_e, \quad (1)$$

$$\rightarrow e_s(\theta) + AB^{**}, \quad (2)$$

where e_i, e_s, and e_e are the incident, scattered, and ionized electrons, respectively; AB and $AB^{**}$are the target molecules in ground state and superexcited state, respectively; θ is the scattering angle of electron in the collision process; $[AB^{n+}]^j$ is a singly or multiply charged ion ($n \geq 1$) in state j which may be stable or decay into different daughter fragments:[1]

$$[AB^{n+}]^j \rightarrow AB^{n+}, \quad (3)$$

$$\rightarrow A^{p+} + B^{q+}. \quad (4)$$

Here, $p+q=n$, and $0 \leq p,q \leq n$. The decay pathways of the molecule AB^{**} in the superexcited state are more abundant:

$$AB^{**} \rightarrow AB^+ + e^-, \quad (5)$$

$$\rightarrow A^* + B,$$

$$\rightarrow A + B + h\nu, \quad (6)$$

$$\rightarrow A^+ + B^-, \quad (7)$$

$$\rightarrow AB'. \quad (8)$$

The processes (5)–(8) represent the autoionzation, neutral dissociation followed by fluorescence emission, ion pair, and other decay processes. Among them, the process (8) is minor and the decay pathways of processes (5) and (6) are dominant, and there is a competition between them, especially for the energy region from the first ionization threshold to about 20 eV.[1] The structured ionization region can also be accessed by an optical method such as the photoabsorption and photoionization method:

$$h\nu + AB \rightarrow [AB^{n+}]^j + ne_e, \quad (9)$$

$$\rightarrow AB^{**}. \quad (10)$$

Then $[AB^{n+}]^j$ and AB^{**} can decay by similar processes as shown in processes (3)–(8). Compared with the electron impact method as shown in processes (1) and (2), in which the momentum transfer can be varied according to different scattering angles of the scattered electron, the momentum transfer

*Project supported by the National Natural Science Foundation of China (Grants Nos. 10734040, 11274291, 10979040, and 11074299), the National Basic Research Program of China (Grant No. 2010CB923301), the Research Fund for the Doctoral Program of Higher Education of China (Grant No. 20103402110027), and the Fundamental Research Funds for the Central Universities, China.

†Corresponding author. E-mail: lfzhu@ustc.edu.cn

© 2013 Chinese Physical Society and IOP Publishing Ltd

of photon to molecule in the optical method is equal to the momentum carried by the photon, which is nearly zero. So the electron impact method can study the momentum transfer dependence behaviors of the structured ionization region including the dipole-allowed and dipole-forbidden superexcited states, as well as their decay processes.

Although numerous investigations have been performed on oxygen, most of them concentrate on the photoabsorption[2–4] and photoionization[5–11] spectral measurements. Among them, the energy level structures of the superexcited states converging to $a^4\Pi_u$, $A^2\Pi_u$, $b^4\Sigma_g^-$, $B^2\Sigma_g^-$, $c^4\Sigma_u^-$, and $C^2\Sigma_u^-$ of oxygen were studied by aforementioned methods based on the double ionization chamber,[2] photoelectron energy spectroscopy,[12] ion mass spectroscopy,[5,8,9] fluorescence spectroscopy,[13–16] and photoelectron–photoion coincidence spectroscopy.[6,7,10,17] The cross sections of the structured ionization region as well as their decay processes were reported in Refs. [7] and [18], which are much less than the investigations of the energy level structures. All aforementioned investigations were carried out by the optical method or dipole (e, e+ion) method, in which the momentum transfer is close to zero. Since the momentum transfer dependence behaviors of different superexcited states are different, some superexcited states may stand out at large scattering angles.[19] However, there are very few investigations[19–21] about the momentum transfer dependence behaviors of the structured ionization region of oxygen. These studies measured the electron energy loss spectra or double differential cross sections at different momentum transfers with incident electron energies of 75 eV,[20] 400 eV,[20] 2500 eV,[19] and 25 keV,[21] besides, some dipole-forbidden superexcited states were also observed and assigned. However, there has been no experimental investigation about the momentum transfer dependence behaviors of the decay processes of the ionization continuum or superexcited states of oxygen.

Many theoretical investigations have been carried out to investigate the "structured" ionization region of oxygen. Most of them deal with the photoionization process, i.e., the electronic partial photoionization cross sections and angular anisotropy factor were calculated.[1] In these calculations, single-channel or single-configuration approximation is generally employed, with Hartree–Fock target wave functions used. In addition, multiple scattering X-alpha (MS-X_α) approximation and *ab initio* static-exchange potentials were also generally used to study the photoionization cross sections of oxygen.[1,22–24] However, these theoretical calculations provide a theoretical insight into photoionization cross sections, rather than to provide quantitatively reliable values.[1] Recently, multichannel configuration-interaction complete-active-space approximation and multichannel Schwinger method with configuration-interaction[25,26] were used to study the electron-correlation effects in photoionization of oxygen, and the calculated photoionization cross sections are in agreement with the experimental ones quantitatively. To the best of our knowledge, the only calculation of the momentum transfer dependence behavior of the superexcited states of oxygen was carried out by Fan *et al*.[19] using the MS-X_α method. However, there has been no theoretical investigation about the momentum transfer dependence behavior of the decay process of the ionization continuum or superexcited states of oxygen.

In this work, the decay pathways of the structured ionization region of oxygen in the different momentum transfers are studied, and this is the first time this issue has been investigated, to the best of our knowledge.

2. Experimental method

In this work, the method of electron–ion coincidence is used. The excitation energy of an atom or molecule can be determined by measuring the difference in energy between the incident electron and scattered electron, and the corresponding experimental setup is called electron energy loss spectrometer (EELS), which is used in this work and described in detail in our previous studies.[27,28] The decay information from the ionization continuum or definite superexcited states to different channels of ion fragments can be obtained by measuring the scattered electrons and ions coincidently. The ions are identified by measuring the time interval from its production to its detection by the time of flight mass spectrometer (TOFMS).

For the present experiment, the setup is operated at an incident electron energy of 2.5 keV and an energy resolution of 80 meV. The mass resolution of TOFMS in this work is about 53 a.m.u. The background pressure in the vacuum chamber is 5×10^{-5} Pa. The true zero angle is calibrated by the symmetry of the angular distribution of the inelastic scattering signals of the transition of $E^3\Sigma_u^-(v'=0)\leftarrow X^3\Sigma_g^-$. The electron energy loss spectra of oxygen and the ion yield spectra of O_2^+ and O^+ were measured at the scattering angles of 0°, 2°, and 4°, and the corresponding energy loss ranges of the spectra at 0°, 2°, and 4° are 8.7 eV–28.4 eV, 11.5 eV–30 eV, and 12.7 eV–67.4 eV, respectively. The energy scales of the measured spectra are calibrated by reference to the $1^1S\rightarrow 2^1P$ transition of helium which occurs at 21.218 eV.

The double differential cross section $d^2\sigma(K,E)/dE\,d\Omega$ of the structured ionization region of oxygen can be determined from the measured energy loss spectra:

$$\frac{d^2\sigma(K,E)}{dE\,d\Omega}=C\cdot N(E), \tag{11}$$

where C is a constant and is determined by counts in 24 eV–26 eV compared with our previously determined double differential cross sections in the same energy region.[19] Then the generalized oscillator strength density (GOSD) $df(K,E)/dE$

of the structured ionization region can be obtained by[29]

$$\frac{\mathrm{d}f(K,E)}{\mathrm{d}E} = \frac{E}{2}\frac{p_0}{p_a}K^2\frac{\mathrm{d}^2\sigma(K,E)}{\mathrm{d}E\,\mathrm{d}\Omega}, \tag{12}$$

where E is the energy loss; p_0 and p_a are the incident and scattered electron momentums, respectively; K is the momentum transfer.

As is well known, for a molecule the relative ionization efficiency generally approaches to a constant and can be normalized to unity when the energy loss is above 20 eV.[1] Therefore, the relative generalized oscillator strength densities of the fragments can be normalized by the same factor. Then the partial generalized oscillator strength density $\mathrm{d}f_{\mathrm{ion}}^{\mathrm{frag}}(K,E)/\mathrm{d}E$ of ion "frag" can be obtained as

$$\frac{\mathrm{d}f_{\mathrm{ion}}^{\mathrm{frag}}(K,E)}{\mathrm{d}E} = \Gamma(K,E)BR^{\mathrm{frag}}(K,E)\frac{\mathrm{d}f(K,E)}{\mathrm{d}E}, \tag{13}$$

where $\Gamma(K,E)$ is the normalized ionization efficiency, and $BR^{\mathrm{frag}}(K,E)$ is the branching ratio of ion "frag" and expressed as

$$BR^{\mathrm{frag}}(K,E) = \frac{N^{\mathrm{frag}}}{\Sigma_{\mathrm{frag}}N^{\mathrm{frag}}}, \tag{14}$$

with N^{frag} being the counts of ion "frag". The ionization GOSD can be obtained by summing the $\mathrm{d}f_{\mathrm{ion}}^{\mathrm{frag}}(K,E)/\mathrm{d}E$ of all ion fragments.

The experimental errors of GOSD or partial GOSD comes mainly from the statistical counts, the normalization procedure of $\mathrm{d}^2\sigma(K,E)/\mathrm{d}E\,\mathrm{d}\Omega$, and $\Gamma(K,E)$. The total experimental error is about 20%∼40% according to the statistical counts of different ions.

3. Results and discussion

Figure 1 shows the GOSD, the ionization GOSD, as well as the partial GOSD, of the structured ionization region 11.8 eV–30 eV of oxygen at $K^2 = 0.23$ a.u. The superexcited states shown in Fig. 1 are assigned according to Refs. [8], [9], [15], [19], [20], and [30], and $R(A)$, $R(a)$, and $R(c)$ represent the ionization thresholds of $A^2\Pi_{\mathrm{u}}$, $a^4\Pi_{\mathrm{u}}$, and $c^4\Sigma_{\mathrm{u}}^-$, respectively. The ionization thresholds of $B^2\Sigma_{\mathrm{g}}^-$, $b^4\Sigma_{\mathrm{g}}^-$, and $C^2\Sigma_{\mathrm{u}}^-$ are also shown in Fig. 1. It can be found from Fig. 1 that the ionization GOSD above 16.8 eV is equal to the GOSD, which is consistent with the previous observation at zero momentum transfer by the dipole (e, e+ion) method that the ionization efficiency approaches to unity when the photon energy is above about 20 eV.[1] Besides the dipole-allowed superexcited states, the dipole-forbidden ones of $(2\sigma_{\mathrm{u}})^{-1}(c^4\Sigma_{\mathrm{u}}^-)np\sigma_{\mathrm{u}}$ (n = 2–6) are also observed in the present spectra at $K^2 = 0.23$ a.u. as shown in Figs. 1 and 2(a), while they are absent in the spectra measured at near zero momentum transfer (Fig. 2(b)). This dipole-forbidden Rydberg series was also observed and assigned by previous electron impact method,[19,20] and the energy positions were reported in these studies. However, there is no investigation into their decay pathway. In order to reveal the decay pathway information of the dipole-forbidden transitions of $(2\sigma_{\mathrm{u}})^{-1}(c^4\Sigma_{\mathrm{u}}^-)np\sigma_{\mathrm{u}}$ (n = 2–6), the spectra in 19 eV–27 eV with good statistics are recorded and shown in Fig. 2. From the previous investigations, the dipole-forbidden superexcited state $(2\sigma_{\mathrm{u}})^{-1}(c^4\Sigma_{\mathrm{u}}^-)2p\sigma_{\mathrm{u}}$ is located at 15.46 eV–16.03 eV,[19] which is less than the appearance potential of O^+, so $(2\sigma_{\mathrm{u}})^{-1}(c^4\Sigma_{\mathrm{u}}^-)2p\sigma_{\mathrm{u}}$ can only decay into O_2^+ (process (5)) or a neutral fragment (process (6)). However, to clarify this question a further study is needed at larger momentum transfer since it has a larger intensity only at a large momentum transfer as observed in Ref. [19]. It can be learnt from Fig. 2(a) that the dipole-forbidden superexcited state of $(2\sigma_{\mathrm{u}})^{-1}(c^4\Sigma_{\mathrm{u}}^-)3p\sigma_{\mathrm{u}}$ can decay into both O_2^+ and O^+ (shown as up-arrow), and these two decay channels have comparable intensities. As for $(2\sigma_{\mathrm{u}})^{-1}(c^4\Sigma_{\mathrm{u}}^-)4p\sigma_{\mathrm{u}}$ (shown as up-arrow in Fig. 2), it is invisible in the spectrum of O_2^+ while it is obvious in the spectrum of O^+, which indicates that $(2\sigma_{\mathrm{u}})^{-1}(c^4\Sigma_{\mathrm{u}}^-)4p\sigma_{\mathrm{u}}$ decays mainly into $O^+ + O$. Because of the poor statistical counts and the limited energy resolution, the decay pathway information of higher dipole-forbidden superexcited state $(2\sigma_{\mathrm{u}})^{-1}(c^4\Sigma_{\mathrm{u}}^-)np\sigma_{\mathrm{u}}$ ($n > 4$) cannot be obtained. More high-resolution experimental investigations are greatly recommended to clarify this problem.

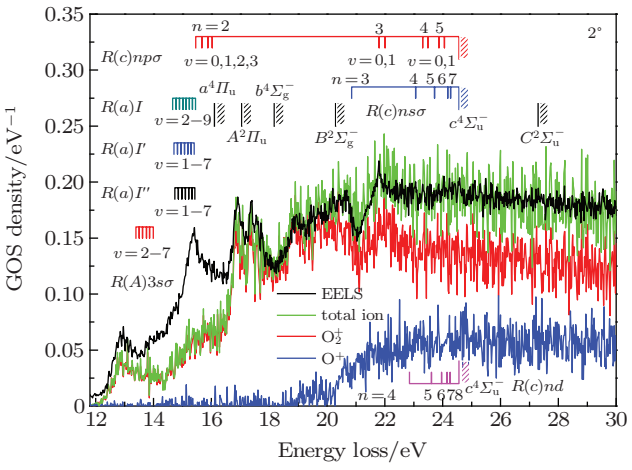


Fig. 1. (color online) The GOSD, ionization GOSD, and partial GOSD, in 11.8 eV–30 eV of oxygen at $K^2 \approx 0.23$ a.u.

In Fig. 2 we can find that each of the spectra at 0° and 2° has a dip in the O_2^+ curve and a shoulder in the O^+ curve (shown as a down-arrow) at 20.3 eV. Because this feature at 0° (near zero momentum transfer) is as obvious as at 2°, it seems not to be a dipole-forbidden superexcited state. From the investigation of photoelectron-photoion coincidence spectroscopy,[7] we can learn that $(3\sigma_{\mathrm{g}})^{-1}B^2\Sigma_{\mathrm{g}}^-$ of O_2^+, whose threshold is 20.3 eV, decays into O^+, and its first four vibronic

states have strong intensities compared with its higher vibronic ones. Therefore, the dip in O_2^+ and the shoulder in O^+ at 20.3 eV should be due to the contribution of ionic dissociation of $B^2\Sigma_g^-$.

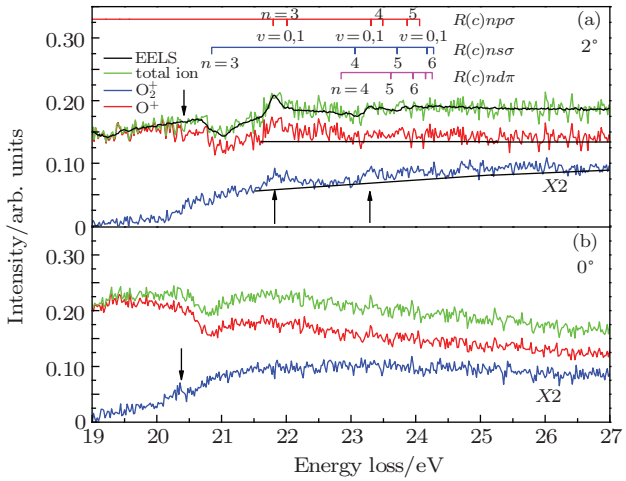


Fig. 2. (color online) The EELS, ion yield spectra measured in 19 eV–27 eV of oxygen at (a) 2° and (b) 0°. The black lines are just used to guide the eyes.

Figure 3 shows the measured spectra at a scattering angle of 4°, i.e., $K^2 \approx 0.91$ a.u. It can be found that there is a feature around 28.8 eV and a broad ridge in 35 eV–65 eV. The former has also been reported in Refs. [19] and [21], and it is assigned as a transition of $(2\sigma_g)^{-1}(1\pi_g)^{3}{}^3\Pi_g \leftarrow X^3\Sigma_g^-$. This transition is dipole-forbidden and quadruple-allowed. Because of the poor statistical counts, we cannot give a clear clarification about its decay pathways.

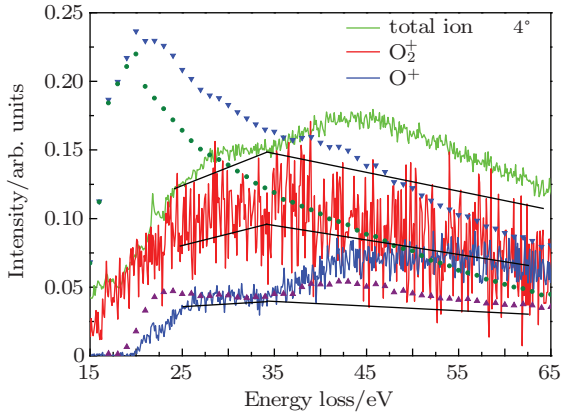


Fig. 3. (color online) The EELS, ion yield spectra in 15 eV–65 eV of oxygen measured at 4°. The black lines are just used to guide the eyes. The curve with symbol ▼ represents the optical oscillator strength density,[18] while ● and ▲ are the partial optical oscillator strength densities of O_2^+ and O^+.[18]

The broad ridge above 35 eV was also reported in Refs. [19] and [21], and it was attributed to the Bethe ridge. However, as is well known, the energy position of the Bethe ridge moves with the variation of the momentum transfer, i.e., $E = K^2/2$.[29] We do not agree with the previous assignment in Refs. [19] and [21] since the maximum of the Bethe ridge should be located at about 12 eV when $K^2 = 0.91$ a.u. at a scattering angle of 4°, which is much less than the broad ridge observed in the present study. In Fig. 3, we also plot the experimental results of Ref. [18], measured by the dipole (e, e+ion) method, in which the momentum transfer is nearly 0. It can be seen clearly that the broad ridge at the same energy position is observed in the spectra measured at 0° and 4°, which indicates that the energy position of the broad ridge is independent of the momentum transfer. Therefore, the broad ridge above 35 eV is not the Bethe ridge. The broad ridge may be caused by the inner-valence excited states of $(2\sigma_g)^{-1}n\lambda$ or multiply excited states. It can be seen clearly from Fig. 3 that the broad ridge has a relatively large intensity at a larger momentum transfer such as at 4°, and it decays mainly into $O^+ + O$.

4. Conclusion

The electron energy loss spectra and ion yield curves at the scattering angles of 0°, 2°, and 4° of O_2 are measured at an incident electron energy of 2500 eV and an energy resolution of 80 meV. Besides the dipole-allowed superexcited states, the dipole-forbidden superexcited states are observed, and their decay pathways at different momentum transfers are measured. It is found that the dipole-forbidden superexcited states of $(2\sigma_u)^{-1}(c^4\Sigma_u^-)np\sigma_u\ {}^3\Sigma_g^- \leftarrow X^3\Sigma_g^-$ decay into different channels according to the principal quantum number n. The broad ridge above 35 eV, which may be caused by the inner-valence excited states of $(2\sigma_g)^{-1}n\lambda$ or multiply excited states, is observed both at small momentum transfer and at large momentum transfer, and its decay channel of $O^+ + O$ is dominant. We hope this work will motivate the theoretical investigation of the momentum transfer dependence behaviors of the decay processes of the ionization continuum or superexcited states of oxygen, which is absent up to now, to the best of our knowledge. We notice that recently the mechanism of ion-pair dissociation of the superexcited state of F_2 was unveiled by the multichannel quantum defect theory,[31,32] and we hope this kind of theoretical method can be extended to the study of the momentum transfer dependence behaviors of the decay processes of the ionization continuum or superexcited states of oxygen.

References

[1] Gallagher J W, Brion C E, Samson J A R and Langhoff P W 1988 *J. Phys. Chem. Ref. Data* **17** 9
[2] Holland D M P, Shaw D A, McSweeney S M, MacDonald M A, Hopkirk A and Hayes M A 1993 *Chem. Phys.* **173** 315
[3] Huffman R E, Larrabee J C and Tanaka Y 1964 *J. Phys. Chem.* **40** 356
[4] Codling K and Madden R P 1965 *J. Chem. Phys.* **42** 3935
[5] Dehmer P M and Chupka W A 1975 *J. Chem. Phys.* **62** 4525
[6] Eland J H D and Duerr E J 1998 *Chem. Phys.* **229** 1
[7] Akahorit T, Moriokat Y, Watanabet M, HayaishiS T, Ito K and Nakamurat M 1985 *J. Phys.* B **18** 2219

[8] Nishitani E, Tanaka I, Tanaka K, Kato T and Koyano I 1984 *J. Chem. Phys.* **81** 3429
[9] Hayaishii T, Iidat Y, Morioka O Y, Sasanumall M, Ishiguro E and Nakamura M 1986 *J. Phys.* B **19** 2861
[10] Ellis K, Hall R I, Avaldi L, Dawber G, McConkey A, Andric L and King G C 1994 *J. Phys.* B **27** 3415
[11] Hao Y S, Zhou C and Mo Y X 2005 *J. Phys. Chem.* A **109** 5832
[12] Baltzer P, Wannberg B, Karlsson L, Gothe M C and Larsson M 1992 *Phys. Rev.* A **45** 4374
[13] Liebel H, Muller-Albrecht R, Lauer S, Vollweiler F, Ehresmann A and Schmoranzer H 2001 *J. Phys.* B **34** 2581
[14] Ehresmann A, Liebel H, Schmoranzer H, Wilhelmi O, Zimmermann B and Schartner K H 2004 *J. Phys.* B **37** 389
[15] Liebel H, Ehresmann A, Schmoranzer H, Demekhin P V, Lagutin B M and Sukhorukov V L 2002 *J. Phys.* B **35** 895
[16] Ukai M, Machida S, Kameta K, Kitajima M, Kouchi N, Hatano Y and Ito K 1995 *Phys. Rev. Lett.* **74** 239
[17] Tang X F, Zhou X G, Niu M L, Liu S L and Sheng L S 2011 *J. Phys. Chem.* A **115** 6339
[18] Brion C E and Tan K H 1979 *J. Electron. Spectrosc. Relat. Phenom.* **17** 101
[19] Fan L L, Zhong Z P, Zhu L F, Liu X J, Yuan Z S, Sun J M and Xu K Z 2005 *Phys. Rev.* A **71** 032704
[20] Dillon M A and Spence D 1981 *J. Chem. Phys.* **74** 6070
[21] Lee J S 1977 *J. Chem. Phys*. **67** 3998
[22] Dittman P M, Dill D and Dehmer J L 1982 *J. Chem. Phys.* **76** 5703
[23] Braunstein M and McKoy V 1988 *J. Chem. Phys*. **90** 3931
[24] Braunstein M and McKoy V 1989 *J. Chem. Phys.* **91** 150
[25] Stratmann R E and Lucchese R R 1995 *J. Chem. Phys.* **102** 8493
[26] Lin P and Lucchese R R 2002 *J. Chem. Phys.* **116** 8863
[27] Wu S L, Zhong Z P, Feng R F, Xing S L, Yang B X and Xu K Z 1995 *Phys. Rev.* A **51** 4494
[28] Liu X J, Zhu L F, Jiang X M, Yuan Z S and Cai B 2001 *Rev. Sci. Instrum.* **72** 3357
[29] Inokuti M 1971 *Rev. Mod. Phys.* **43** 297
[30] Krupenie P H 1972 *J. Phys. Chem. Ref. Data* **1** 423
[31] Gao X, Zhang W H, Mo Y X and Li J M 2010 *Phys. Rev.* A **82** 031401
[32] Zhang W H, He C L, Hao Y S, Mo Y X and Li J M 2007 *Chin. Phys. Lett.* **24** 1220